Check for updates

Effectiveness of beetroot seeds and H_3PO_4 activated beetroot seeds for the removal of dyes from aqueous solutions

A. Machrouhi, M. Farnane, A. Elhalil, R. Elmoubarki, M. Abdennouri, S. Qourzal, H. Tounsadi and N. Barka

ABSTRACT

Raw beetroot seeds (BS) and H_3PO_4 activated beetroot seeds (H_3PO_4-BS) were evaluate for their effectiveness in removing methylene blue (MB) and malachite green (MG) from aqueous solution. BS were carbonized at 500°C for 2 h, and then impregnated with phosphoric acid (phosphoric acid to BS ratio of 1.5 g/g). The impregnated BS were activated in a tubular vertical furnace at 450°C for 2 h. Batch sorption experiments were carried out under various parameters, such as solution pH, adsorbent dosage, contact time, initial dyes concentration and temperature. The experimental results show that the dye sorption was influenced by solution pH and it was greater in the basic range. The sorption yield increases with an increase in the adsorbent dosage. The equilibrium uptake was increased with an increase in the initial dye concentration in solution. Adsorption kinetic data conformed more to the pseudo-second-order kinetic model. The experimental isotherm data were evaluated by Langmuir, Freundlich, Toth and Dubinin–Radushkevich isotherm models. The Langmuir maximum monolayer adsorption capacities were 61.11 and 74.37 mg/g for MB, 51.31 and 213.01 mg/g for MG, respectively in the case of BS and H_3PO_4-BS. The thermodynamic parameters are also evaluated and discussed.

Key words | activated beetroot seeds, dye removal, equilibrium, kinetics, thermodynamics

A. Machrouhi
M. Farnane
A. Elhalil
R. Elmoubarki
M. Abdennouri
N. Barka (corresponding author)
Laboratoire des Sciences des Matériaux, des Milieux et de la Modélisation (LS3M), FPK, Univ Hassan 1, B.P. 145, Khouribga 25000, Morocco
E-mail: *barkanoureddine@yahoo.fr*

S. Qourzal
Equipe de Catalyse et Environnement, Département de Chimie, Faculté des Sciences, Université Ibn Zohr, B.P.8106 Cité Dakhla, Agadir, Morocco

H. Tounsadi
Faculté des Sciences Dhar El Mahraz, Université Sidi Mohamed Ben Abdellah, Fès, Morocco

INTRODUCTION

The contamination of natural and industrial waters by textile dyes is now recognized as a major environmental concern. These environmental problems may be due to the rapid development of various industries, such as textile, paper, leather, coating, cosmetic and plastic. Among the 7×10^5 tons and 10,000 different types of dyes and pigments produced globally every year, it has been estimated that 1–15% of dyes were expelled in the effluents during the dyeing process (Zollinger 1991). This massive influx of untreated organic chemicals into waterways not only gives rise to aesthetic concerns, but far more importantly it promotes eutrophication and adversely affects environmental conditions. Due to their persistence and their refractory carcinogenic nature, dyes represent an increasing environmental danger (Reife 1993). In order to protect the environment, synthetic dyes should be removed from wastewaters.

A wide variety of techniques have been used for dye removal from wastewaters including biological degradation (Santos *et al.* 2007), photodegradation (Abaamrane *et al.*

This is an Open Access article distributed under the terms of the Creative Commons Attribution Licence (CC BY 4.0), which permits copying, adaptation and redistribution, provided the original work is properly cited (http://creativecommons.org/licenses/by/4.0/).

doi: 10.2166/wrd.2017.034

Downloaded from http://iwaponline.com/jwrd/article-pdf/8/4/522/482431/jwrd0080522.pdf
by guest

2012), coagulation (Sureshkumar & Namasivayam 2008), membrane filtration (Wu *et al.* 1998), reverse osmosis (Ravikumar *et al.* 2007) and adsorption (Elmoubarki *et al.* 2016) or a synergic combination of different methods. Among these water purification and recycling technologies, adsorption is generally a fast, less expensive and widely applicable method. Several low-cost adsorbents have been reported to reduce dye concentrations from aqueous solutions, including agricultural waste (Ahmad *et al.* 2014; Anastopoulos & Kyzas 2014), lignite (Gurses *et al.* 2014), sugar waste (Anastopoulos *et al.* 2017), synthetic clays (Elmoubarki *et al.* 2017), chitosan (Tsai *et al.* 2014), silica (Zarezadeh-Mehrizi & Badiei 2014), kaolinite (Dogan *et al.* 2009), perlite (Dogan & Alkan 2003), sepiolite (Ozdemir *et al.* 2006), montmorillonite (Gemeay *et al.* 2002) and ball clay (El Ouardi *et al.* 2017), and some natural biosorbents have also been tested (Tounsadi *et al.* 2016). These materials generally have low sorption efficiencies and therefore, a large adsorbent dosage is necessary to remove a low dye concentration. In order to enhance the performance efficiency of the sorption processes, it is necessary to develop cheaper, easily available adsorbents with great sorption capacities. In particular, the use of lignocellulosic biomass is a promising alternative adsorbent due to its relative abundance, availability and low commercial value.

Beetroot seeds (BS) are a cheap, abundantly available and renewable precursor. Their high ligno-cellulosic content makes them an efficient precursor for the preparation of activated carbon. Preparation involves treatment with H_3PO_4 which acts as a dehydrating catalyst, promoting decomposition of the cellulosic precursor at a lower heat treatment temperature. The presence of H_3PO_4 in the interior of the precursor restricts tar formation and inhibits the shrinkage of the precursor particle by occupying a substantial volume resulting in the lower weight loss and higher yield for H_3PO_4 impregnated carbon (Ahmad & Thyodan 2013).

The aim of the present work was to evaluate the ability of BS and H_3PO_4 activated beetroot seeds (H_3PO_4-BS) to adsorb methylene blue (MB) and malachite green (MG) from aqueous solution. Various parameters were studied in batch adsorption including the effect of solution pH, adsorbent dosage contact time, initial dye concentration and temperature. For adsorption kinetic modelling, two kinetic models (pseudo-first-order and pseudo-second-order kinetics) were used, and four isotherm models (Langmuir, Freundlich, Toth and Dubinin–Radushkevich) were applied to fit the experimental equilibrium data. The thermodynamics of the adsorption was also analysed.

METHODS AND MATERIALS

Materials

All the chemicals used in this study were of analytical grade. The dyes MB and MG were obtained from Sigma-Aldrich and used without further purification. The chemical formulae and some other specific characteristics of these dyes are summarized in Table 1.

Preparation and characterization of the adsorbents

Locally obtained BS were repeatedly washed with distilled water to remove dirt particles and were then dried at 80°C for 24 h. The dried seeds were further powdered using a domestic mixer. Ten grams powdered BS were pyrolysed at 500°C for 2 h under a nitrogen atmosphere. The char obtained was impregnated with phosphoric acid (purity 85%, Acros Organics) at phosphoric acid to BS ratio of 1.5 for 6 h, and followed by the removal of excess solution and overnight drying at 110°C. Then, the char sample was activated at 450°C for 2 h. Subsequently, the cooled samples were repeatedly washed with hot deionized water to remove free phosphoric acid, tar, fines and leachable matter followed by overnight drying at 110°C.

Adsorption tests

Dye solutions were prepared by dissolving desired amounts of each dye in distilled water and required concentrations were obtained by dilution. Sorption experiments in batch mode were carried out in a series of 50 mL beakers containing the required weight of each adsorbent and 50 mL of the dye solution at the indicated concentration and constantly agitated at 350 rpm. Effect of test conditions were investigated by varying pH of the solution from 2 to 10, adsorbents dosage from 0.25 to 6 g/L and contact time

Downloaded from http://iwaponline.com/jwrd/article-pdf/8/4/522/482431/jwrd0080522.pdf
by guest

Table 1 | Physicochemical characteristics of the dyes used

Name	Molecular structure	M_W (g/mol)	λ_{max} (nm)
MB (Basic blue 9)	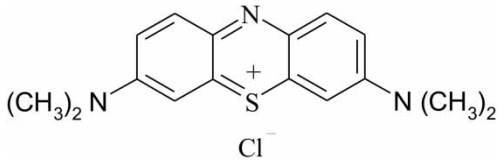	319.85	661
MG (Basic green 4)	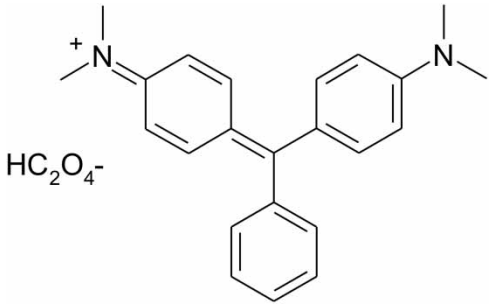	329.5	621

from 5 to 240 min. The influence of initial dye concentration was also established over the range of 20 to 200 mg/L. The temperature was varied from 10°C to 50°C under otherwise optimum conditions. The solution pH was adjusted by adding NaOH (0.1 N) or HNO_3 (0.1 N) and measured by a sensION+ PH31 pH metre. The temperature was controlled using a thermostatically controlled incubator.

After sorption experiments were completed, samples were withdrawn and centrifuged at 3,000 rpm for 10 min. The residual concentrations were further determined from UV-Vis characteristics at maximum absorption wavelength of each dye using a TOMOS V-1100 UV-vis spectrophotometer.

The adsorption efficiency and adsorption yield were calculated using Equations (1) and (2):

$$q = \frac{(C_0 - C)*\mathrm{V}}{m} \quad (1)$$

$$\%\ \text{Removal} = \frac{(C_0 - C)}{C_0}*100 \quad (2)$$

where q (mg/g) is the adsorption quantity, C_0 (mg/L) is the initial dye concentration, C (mg/L) is the dye concentration, m (g) is the mass of adsorbents and V (L) is volume of dye solution.

RESULTS AND DISCUSSION

Fourier transform infrared spectroscopy

Fourier transform infrared (FTIR) spectra of BS and H_3PO_4-BS are given in Figure 1. The broad peaks in the 3,600–2,900, 1,700–1,400 and 1,300–900 cm^{-1} ranges indicative of existence of various functional groups that can participate in sorption process. FTIR spectrum of BS shows a strong band between 3,600 and 3,200 cm^{-1} due to overlapping of

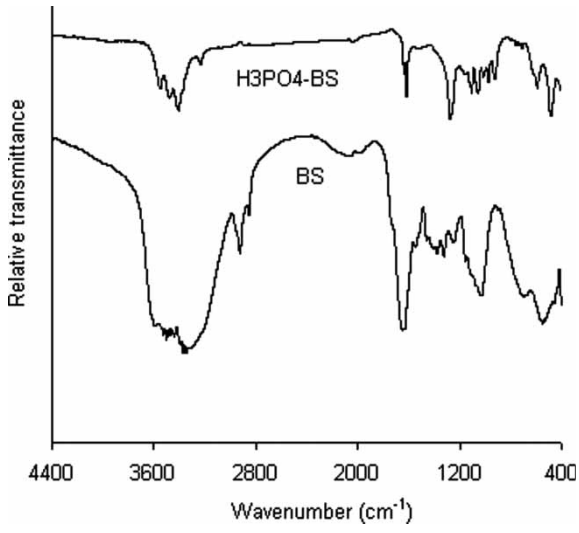

Figure 1 | FTIR spectra of BS and H_3PO_4-BS adsorbents.

Downloaded from http://iwaponline.com/jwrd/article-pdf/8/4/522/482431/jwrd0080522.pdf
by guest

the hydrogen bond stretching vibration of the hydroxyl groups linked in cellulose, lignin, adsorbed water and amide groups (-NH) (Mas Haris & Sathasivam 2009). After activation, this band was separated into three more resolved bands: two bands at around 3,300 and 3,250 cm^{-1} are ascribable to vibrations of hydroxyl groups, whereas the position of the band for non-bonded alcohols, phenols and carboxylic acids is usually around 3,500 cm^{-1}. The bands at 2,920–2,800 cm^{-1} are attributed to aliphatic C–H stretching vibrations in an aromatic methoxyl group, in methyl and methylene groups of side chains. These bands were observed as much stronger in raw BS; they were not seen in the FTIR spectrum of H_3PO_4-BS. The bands at 1,600 cm^{-1} are characteristic of C = O stretching vibrations of ketones, aldehydes, lactones or carboxyl groups. These bands become finer in the H_3PO_4-BS. The bands between 1,590 and 1,400 cm^{-1} are usually ascribed to C = C vibrations, although some overlapping can be found with δ (O–H) around 1,450 cm^{-1}. The bands at about 1,020 cm^{-1} are attributed to C–O–C stretching (alcohols, ethers or phenols) and O–H deformation vibrations (Foo & Hameed 2011). These bands were decreased by the activation process as compared to the raw material.

For H_3PO_4-BS, the appearance of additional peaks between 800 and 700 cm^{-1} may be due to the interaction of phosphorous species resulting from phosphoric acid activation (Guo & Rockstraw 2006). However, H_3PO_4 can also produce activation through the formation of phosphate and polyphosphate bridges which connect crosslink biopolymer fragments, avoiding the contraction of the material. The removal of the activating agent during washing leads to a matrix in an expanded state with an accessible pore structure (Kennedy *et al.* 2004).

Effect of pH on dyes adsorption

The pH of the solution is an important parameter affecting the surface charge of the adsorbents as well as the degree of ionization of different pollutants. This subsequently leads to a shift in reaction equilibrium characteristics of adsorption process. Figure 2 shows the effect of pH from 2 to 10 on the adsorption quantity (q_e) of MB and MG onto BS and H_3PO_4-BS. It can be seen that the adsorption is weak in acidic medium. As the pH increases, the adsorption capacities increase. This result may be due to alterations in the

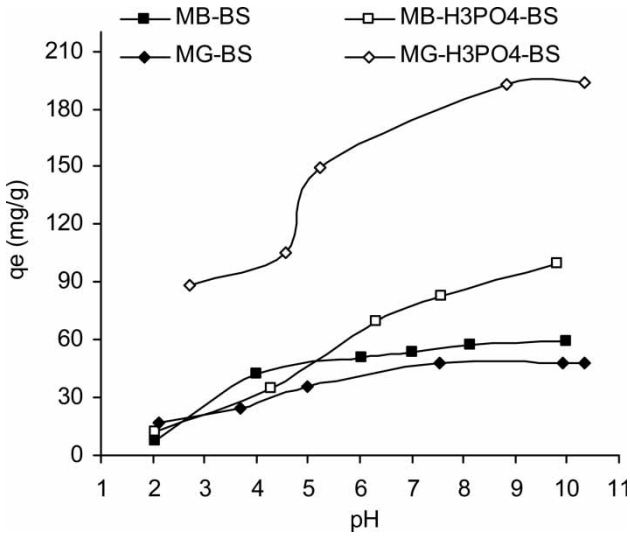

Figure 2 | Effect of pH on the adsorption of MB and MG onto BS and H_3PO_4-BS: C_0 = 100 mg/L, contact time = 120 min, R = 0.5 g/L, T = 25°C.

adsorbent's surface charge or in the charge state of dyes. The pH values of zero charge (pH_{PZC}) of the adsorbents were found to be 6.2 and 4.7, respectively, for BS and H_3PO_4-BS. At pH values above this point, the high sorption of dyes may be explained as occurring on the negative sites, and the ionic state of functional groups such as carboxyl, phosphoryl, sulfhydryl, hydroxyl and amino will be such as to promote reaction with MB and MG as cationic dyes. The optimal values of pH used in the further experiment were identified as pH = 5.00 for MG and pH = 6.05 for MB.

Effect of adsorbent dosage

Adsorbent dosage is a highly influential parameter in sorption processes. It determines the capacity of an adsorbent for a given initial concentration of dye molecules. Data obtained from the experiments with varying adsorbent dosage or mass ratio (R) are presented in Figure 3. It shows that the sorption yield significantly increased with an increase of the amount of BS or H_3PO_4-BS. For BS, the adsorption yield increased from 30.3% to 86.1% for MB and from 23.2% to 90.5% for MG, when the adsorbent dosage was increased from 0.5 to 4 g/L. For H_3PO_4-BS, the adsorption yield increased from 43.4% to 98.7% for MB and from 69.3% to 96.6% for MG, when the adsorbent dosage was increased from 0.25 to 2 g/L. The observed

Downloaded from http://iwaponline.com/jwrd/article-pdf/8/4/522/482431/jwrd0080522.pdf
by guest

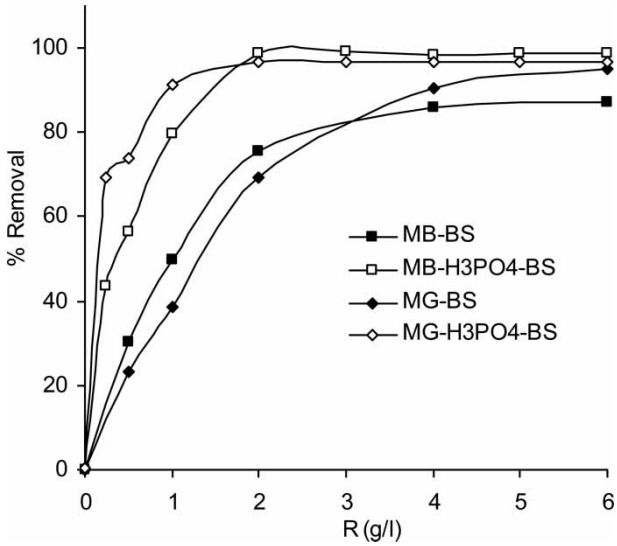

Figure 3 | Effect of adsorbent dosage or mass ratio (R) on the removal of MB and MG by BS and H_3PO_4-BS: $C_0 = 100$ mg/L, contact time = 120 min, initial pH = 6.15 (MB), 5.45 (MG), T = 25°C.

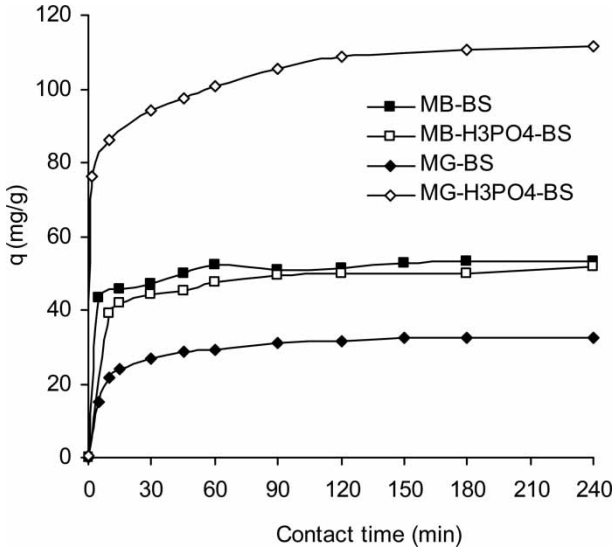

Figure 4 | Kinetics of MB and MG adsorption by BS and H_3PO_4-BS: $C_0 = 100$ mg/L, R = 0.5 g/L, initial pH = 6.15 (MB), 5.45 (MG), T = 25°C.

enhancement in adsorption yield with increasing adsorbent concentration could be mainly due to greater available possible binding sites and surface area of the adsorbents. A further increase in adsorbent dosage over 2 g/L for H_3PO_4-BS and 4 g/L for BS did not lead to a significant improvement in adsorption yield. This lack of improvement may be a consequence of a partial aggregation of adsorbent particles, which results in a decrease in effective surface area for the biosorption. Figure 3 shows that activation of BS strongly enhances adsorption potential for the selected dyes. Further, the optimal value of adsorbent dosage used in the following experiment was 0.5 g/L for both adsorbents in the removal of the both dyes.

Adsorption kinetics

The plot of MB and MG adsorption versus contact time is shown in Figure 4. The uptake of MB and MG increased quickly in the first period of the process and then the rate of biosorption slowed and stagnated with the increase in contact time. The equilibrium time was 60 min for the adsorption of BM by both adsorbents and was 120 min in the case of MG. In order to describe the kinetics involved in MB and MG sorption, two commonly used kinetic models – pseudo-first order and pseudo-second order rate equations – were applied to fit the kinetic data. This analysis is based on the regression coefficient (r^2) and the amount of dye adsorbed per unit weight of the adsorbent.

The first-order rate expression of Lagergren based on solid capacity is generally reported as in Equation (3) (Lagergren 1898):

$$q = q_e(1 - e^{-k_1 t}) \tag{3}$$

where q_e and q (both in mg/g) are respectively the amounts of dye adsorbed at equilibrium and at any time t, and k_1 (1/min) is the rate constant of adsorption.

The pseudo-second-order model proposed by Ho & McKay (1998) was used to characterize the sorption kinetics. This model is based on the assumption that the adsorption follows second-order chemisorption (Blanchard *et al.* 1984). The pseudo-second-order model can be represented as:

$$q = \frac{k_2 q_e^2 t}{1 + k_2 q_e t} \tag{4}$$

where k_2 (g/mg·min) is the rate constant of pseudo-second-order adsorption.

Parameters of the pseudo-first-order and pseudo-second-order models were evaluated by non-linear regression. The data and the correlation coefficients, r^2, are summarized in Table 2: the correlation coefficients for the pseudo-second-order kinetic model are closer to 1 than that of the

Downloaded from http://iwaponline.com/jwrd/article-pdf/8/4/522/482431/jwrd0080522.pdf
by guest

Table 2 | Kinetic constants for MB and MG adsorption onto BS and H_3PO_4-BS

			Pseudo-first-order			Pseudo-second-order		
Adsorbent	**Dye**	q_{exp} (mg/g)	q_e (mg/g)	k_1 (1/min)	r^2	q_e (mg/g)	k_2 (g/mg·min)	r^2
BS	MB	52.98	50.72	0.373	0.976	52.04	0.0153	0.990
	MG	32.51	30.79	0.115	0.973	33.04	0.0052	0.997
H_3PO_4-BS	MB	51.87	48.33	0.150	0.978	50.69	0.0059	0.994
	MG	111.36	101.89	0.681	0.943	104.69	0.0103	0.967

Lagergren first order. It can be concluded from this result that the sorption mechanism of MB and MG follows the pseudo-second-order model rather than the Lagergren first order for the systems investigated in this work. As dye adsorption is described by pseudo-second-order kinetics, this indicates that boundary layer resistance was not the rate limiting step (Slimonin 2016). These results suggest that the dye adsorption may be controlled generally by a chemisorption process via ion exchange and/or a complexation process, in conjunction with the chemical characteristics of the adsorbent and the dyes (Eren & Acar 2006).

Adsorption isotherms

Equilibrium adsorption experiments were conducted by evaluating the sorption capacity of BS and H_3PO_4-BS for MB and MG for different initial dye concentrations. The results are shown in Figure 5 and indicate that adsorption efficiencies of both dyes increase with increasing of the initial concentration of dyes. When the initial concentration increased, the driving force for mass transfer becomes larger, resulting in higher adsorption. Thus, high concentration of MB and MG in solution implicates a high concentration of molecules fixed at the surface of the adsorbents. Langmuir, Freundlich, Toth and Dubinin–Radushkevich models were applied for the analysis of equilibrium sorption data obtained.

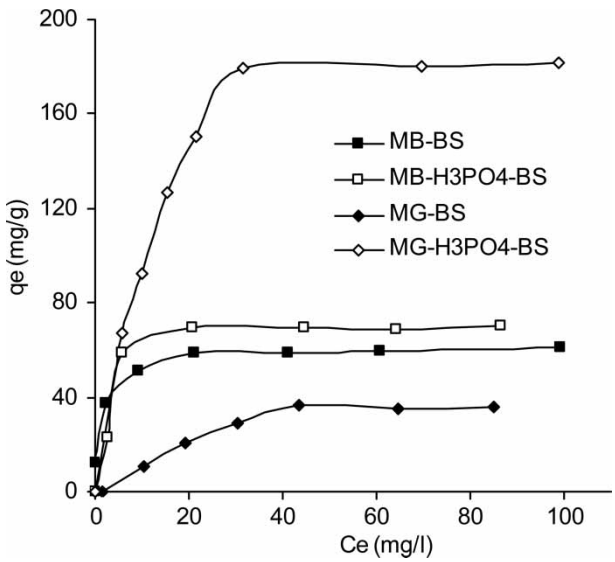

Figure 5 | Adsorption isotherms of MB and MG onto BS and H_3PO_4-BS: contact time = 120 min, R = 0.5 g/L, initial pH = 6.15 (MB), 5.45 (MG), T = 25°C.

Langmuir model

The Langmuir (1916) isotherm model assumes that the adsorption occurred in a monolayer with uniformly energetic adsorption sites and no lateral interaction between adsorbed molecules. Therefore, at equilibrium, a saturation point is reached where no further adsorption can occur. A basic assumption is that sorption takes place at specific homogeneous sites within the adsorbent. The expression formula of the Langmuir isotherm is given by Equation (5):

$$q_e = \frac{q_m K_L C_e}{1 + K_L C_e} \tag{5}$$

where q_e(mg/g) is the adsorbed amount at equilibrium, C_e is the equilibrium dye concentration (mg/L), K_L is Langmuir equilibrium constant (L/mg) and q_m the maximum adsorption capacity (mg/g).

Freundlich model

The Freundlich isotherm model deals with sorption at a heterogeneous surface and sites with different energy of adsorption. The energy of adsorption changes as function of surface coverage (Freundlich & Heller 1939). The

Downloaded from http://iwaponline.com/jwrd/article-pdf/8/4/522/482431/jwrd0080522.pdf
by guest

Freundlich equation is expressed by Equation (6). This equation can also fit multilayer sorption.

$$q_e = K_F C_e^{1/n} \quad (6)$$

where K_F is the Freundlich constant and n is the heterogeneity factor.

The K_F value is related to the adsorption capacity; while $1/n$ value is dependent to the adsorption intensity.

Toth model

To reduce the error between experimental data and predicted values of equilibrium adsorption data by modification of the Langmuir equation, the Toth model was introduced (Toth 2000). This model assumes a quasi-Gaussian energy distribution. The application of this equation is best suited to multilayer adsorption similar to BET (Brunauer, Emmet and Teller) isotherms. This represents a special type of Langmuir isotherm and has very restricted validity (Khan *et al.* 1997). The Toth correlation is given as:

$$q_e = \frac{q_m C_e}{(1/K_T + C_e^t)^{1/t}} \quad (7)$$

where q_e is the adsorbed amount at equilibrium (mg/g), C_e the equilibrium concentration of the adsorbate (mg/L), q_m the Toth maximum adsorption capacity (mg/g), K_T the Toth equilibrium constant and t is the Toth model exponent. If the exponent t is equal to unity, the model of Toth can be reduced to the Langmuir model.

Dubinin–Radushkevich model

The Dubinin–Radushkevich isotherm is a more general model than Langmuir model, although, it does not assume a homogenous surface or constant sorption potential. The Dubinin–Radushkevich isotherm equation is given by Equations (8) and (9) (Dubinin & Radushkevich 1947):

$$q_e = q_m \exp(-B\varepsilon^2) \quad (8)$$

$$\varepsilon^2 = RT \ln\left(1 + \frac{1}{C_e}\right) \quad (9)$$

where B is a constant related to the adsorption energy, q_m is the theoretical saturation capacity and ϵ is the Polanyi potential.

Analysis of adsorption isotherms

The constant parameters of the isotherm models were evaluated by nonlinear regression analysis of the experimental adsorption isotherms obtained and the adsorption isotherm models. After analysis, the data with correlation coefficients (r^2) are shown in Table 3. It can be seen that the equilibrium data conform well to the Toth model with high correlation coefficients. The Langmuir model also yielded a good fit to experimental data with maximum monolayer adsorption capacities of 61.11 and 74.37 mg/g for MB, 51.31 and 213.01 mg/g for MG, respectively in the case of BS and H_3PO_4-BS. The increase in dye sorption is related to the cation exchange capacity after activation of BS with H_3PO_4 due to the formation of more functional groups. From these results, it can be concluded that the activation enhances the adsorption capacity of BS more strongly for MG than for MB.

Effect of temperature

The effect of temperature on the adsorption of MB and MG was tested, bearing in mind the specific

Table 3 | Isotherm model constants for the adsorption of MB and MG onto BS and H_3PO_4-BS

	Langmuir				Freundlich			Toth				Dubinin–Radushkevich		
Dye	Adsorbent	q_m	K_L	r^2	K_F	n	r^2	q_m	K_T	t	r^2	q_m	B	r^2
MB	BS	61.11	0.702	0.972	32.16	6.31	0.956	74.20	2.991	0.359	0.993	58.92	0.00034	0.936
	H_3PO_4-BS	74.37	0.308	0.936	35.92	6.39	0.856	69.72	8.26E-8	8.386	0.989	74.14	0.00111	0.855
MG	BS	51.31	0.036	0.950	4.64	2.04	0.878	36.01	1.45E-11	7.02	0.995	45.35	0.00597	0.979
	H_3PO_4-BS	213.01	0.094	0.974	57.39	3.68	0.912	185.07	0.0008	2.486	0.993	203.78	0.00292	0.962

Downloaded from http://iwaponline.com/jwrd/article-pdf/8/4/522/482431/jwrd0080522.pdf
by guest

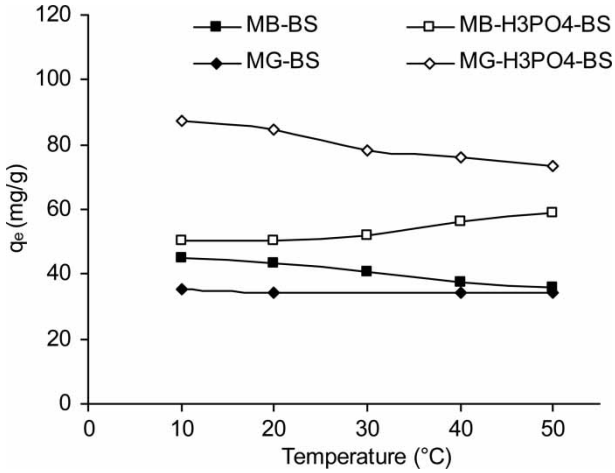

Figure 6 | Effect of temperature on the adsorption of MB and MG by BS and H_3PO_4-BS. $C_0 = 100$ mg/L, R = 0.5 g/L, initial pH = 6.15 (MB), 5.45 (MG).

circumstances of dyestuff wastes in different kinds of effluents. Data were collected at five temperatures from 10°C to 50°C. The variation of adsorbed quantities versus solution temperature is illustrated in Figure 6. It can be seen that the amount of MB adsorbed on BS decreases when the temperature increases, whereas the amount of MG adsorbed by the same adsorbent was not affected by changes in solution temperature. For H_3PO_4-BS, an increase in the amount of MB adsorbed was observed with rise in temperature. This result may be due to various factors such as enhancement of interaction between adsorbent and MB, creation of new adsorption sites and increased rate of intra-particle diffusion at higher temperatures. However, this is not the case in MG adsorption which was strongly decreased by increasing solution temperature from 20°C to 50°C.

To describe thermodynamic behaviour of the adsorption of MB and MG thermodynamic parameters including the change in free energy (ΔG°), enthalpy (ΔH°) and entropy (ΔS°) were used. These parameters were determined according to the following reversible process (Bakas *et al.* 2014):

$$\text{dye in solution} \rightleftharpoons \text{adsorbed dye} \tag{10}$$

For such equilibrium reactions, K_D, the distribution constant, can be expressed as:

$$K_D = \frac{q_e}{C_e} \tag{11}$$

The Gibbs free energy is:

$$\Delta G^\circ = -RT \ln(K_D) \tag{12}$$

where R is the universal gas constant (8.314 J mol/K) and T is solution temperature in K.

The enthalpy (ΔH°) and entropy (ΔS°) of adsorption were estimated from the slope and intercept of the plot of ln K_D versus $1/T$ yields, respectively.

$$\text{Ln}\, K_D = -\frac{\Delta G^\circ}{RT} = -\frac{\Delta H^\circ}{RT} + \frac{\Delta S^\circ}{R} \tag{13}$$

As shown in Table 4, because the values of ΔG° are negative at different temperatures, the adsorption of dyes

Table 4 | Thermodynamic parameters calculated for the adsorption of the dyes by BS and H_3PO_4-BS

		MB					MG				
Adsorbent	**T°C**	**q_e (mg/g)**	**K_D**	**ΔG° (J/mol)**	**ΔH° (kJ/mol)**	**ΔS° (J/K·mol)**	**q_e (mg/g)**	**K_D**	**ΔG° (J/mol)**	**ΔH° (kJ/mol)**	**ΔS° (J/K·mol)**
BS	10	44.85	4.36	−3462.69	− 24.95	− 75.67	35.09	1.18	−383.12	−1.43	−3.86
	20	43.39	3.28	−2897.08			34.36	1.10	−229.61		
	30	40.83	2.23	−2015.10			36.00	1.29	−633.11		
	40	37.67	1.53	−1103.07			34.22	1.08	−210.14		
	50	35.63	1.24	−576.20			34.18	1.08	−207.81		
H_3PO_4 – BS	10	39.06	0.62	−52.05	33.30	9.79	87.14	1.54	−1022.59	−5.72	−16.53
	20	36.93	0.59	−23.39			84.73	1.47	−938.84		
	30	40.10	0.67	−210.07			78.40	1.29	−640.59		
	40	46.49	0.87	−680.53			76.14	1.23	−537.64		
	50	50.10	1.00	−981.83			73.43	1.16	−399.20		

Downloaded from http://iwaponline.com/jwrd/article-pdf/8/4/522/482431/jwrd0080522.pdf
by guest

is thermodynamically feasible with a spontaneous process (Anastopoulos & Kyzas 2016). All ΔG° values increase with the increase in solution temperature except for adsorption of MB by H_3PO_4-BS, indicating a decrease in feasibility of adsorption at higher temperatures. The enthalpy of adsorption (ΔH°) was found to be −24.95 and 33.30 kJ/mol for MB and −1.43 and −5.72 kJ/mol for MG, respectively, in the case of BS and H_3PO_4-BS. The ΔS° parameter was found to be negative for adsorption of MG by BS and H_3PO_4-BS, which suggests a decrease in the randomness at the solid/solution interface during the adsorption. For the adsorption of MB, ΔS° was found to be negative in the case of BS and positive in the case of H_3PO_4-BS.

CONCLUSIONS

In this study, adsorption experiments for the removal of MB and MG dyes from aqueous solutions have been carried out using raw BS and H_3PO_4 H_3PO_4-BS. The results show that the adsorption was pH dependent with a high adsorption of dye in the basic range. The amount of adsorbed dye increases if the sorbent dose increases by reason of the availability of adsorption sites in the surface of the sorbents. Pseudo-second-order kinetics describe the adsorption kinetic data well. The equilibrium uptake was increased with the rise of the initial dye concentration in solution whereas the adsorption isotherm can be best fitted by the Toth and Langmuir isotherm models. The adsorption capacity of H_3PO_4-BS is more influenced by solution temperature. Thus, BS can be used as an effective precursor for the preparation of activated carbon. In this context, both BS and H_3PO_4-BS might be useful for the treatment of wastewater containing synthetic dyes.

ACKNOWLEDGEMENTS

The authors would like to thank University Hassan I of Settat for financial support of this study.

REFERENCES

Abaamrane, A., Qourzal, S., Barka, N., Mançour-Billah, S., Assabbane, A. & Ait-Ichou, Y. 2012 Optimal decolorization efficiency of indigo carmine by TiO_2/UV photocatalytic process coupled with response surface methodology. *Oriental Journal of Chemistry* **28**, 1091–1098.

Ahmad, M. J. & Thyodan, S. K. 2013 Microwave assisted preparation of microporous activated carbons from Siris seeds pods for adsorption of metronidazole antibiotic. *Chemical Engineering Journal* **214**, 310–318.

Ahmad, M. A., Ahmad Puad, N. A. & Bello, O. S. 2014 Kinetic, equilibrium and thermodynamic studies of synthetic dye removal using pomegranate peel activated carbon prepared by microwave-induced KOH activation. *Water Resources and Industry* **6**, 18–35.

Anastopoulos, I. & Kyzas, G. Z. 2014 Agricultural peels for dye adsorption: a review of recent literature. *Journal of Molecular Liquids* **200**, 381–389.

Anastopoulos, I. & Kyzas, G. Z. 2016 Are the thermodynamic parameters correctly estimated in liquid-phase adsorption phenomena? *Journal of Molecular Liquids* **218**, 174–185.

Anastopoulos, I., Bhatnagar, A., Hameed, B. H., Ok, Y. S. & Omirou, M. 2017 A review on waste-derived adsorbents from sugar industry for pollutant removal in water and wastewater. *Journal of Molecular Liquids* **240**, 179–188.

Bakas, I., Elatmani, K., Qourzal, S., Barka, N., Assabbane, A. & Ait-Ichou, Y. 2014 A comparative adsorption for the removal of *p*-cresol from aqueous solution onto granular activated charcoal and granular activated alumina. *Journal of Materials and Environmental Science* **5**, 675–682.

Blanchard, G., Maunaye, M. & Martin, G. 1984 Removal of heavy metals from waters by means of natural zeolites. *Water Research* **18**, 1501–1507.

Dogan, M. & Alkan, M. 2003 Adsorption kinetics of methyl violet onto perlite. *Chemosphere* **50**, 517–528.

Dogan, M., Karaoglu, M. H. & Alkan, M. 2009 Adsorption kinetics of maxilon yellow 4GL and maxilon red GRL dyes on kaolinite. *Journal of Hazardous Materials* **165**, 1142–1151.

Dubinin, M. M. & Radushkevich, L. V. 1947 The equation of the characteristic curve of the activated charcoal. *Proceedings of the Academy of Sciences, Physical Chemistry Section* **55**, 331–337.

Elmoubarki, R., Moufti, A., Tounsadi, H., Mahjoubi, F. Z., Farnane, M., Machrouhi, A., Elhalil, A., Abdennouri, M., Zouhri, A. & Barka, N. 2016 Kinetics and thermodynamics study of methylene blue adsorption onto Aleppo pine cones. *Journals of Materials and Environmental Science* **7**, 2869–2879.

Elmoubarki, R., Mahjoubi, F. Z., Elhalil, A., Tounsadi, H., Abdennouri, M., Sadiq, M., Qourzal, S., Zouhri, A. & Barka, N. 2017 Ni/Fe and Mg/Fe layered double hydroxides and their calcined derivatives: preparation, characterization and

Downloaded from http://iwaponline.com/jwrd/article-pdf/8/4/522/482431/jwrd0080522.pdf
by guest

application on textile dyes removal. *Journals of Material Research and Technology* **6**, 271–283.

El Ouardi, M., Qourzal, S., Assabbane, A. & Douch, J. 2017 Adsorption studies of cationic and anionic dyes on synthetic ball clay. *Journal of Applied Surfaces and Interfaces* **1** (1–3), 28–34.

Eren, Z. & Acar, F. 2006 Adsorption of Reactive Black 5 from an aqueous solution: equilibrium and kinetic studies. *Desalination* **194**, 1–10.

Foo, K. Y. & Hameed, B. H. 2011 Preparation and characterization of activated carbon from pistachio nut shells via microwave-induced chemical activation. *Biomass Bioenergy* **35**, 3257–3261.

Freundlich, H. & Heller, W. 1939 The adsorption of cis- and trans-azobenzene. *Journal of the American Chemical Society* **61**, 2228–2230.

Gemeay, A. H., El-Sherbiny, A. S. & Zaki, A. B. 2002 Adsorption and kinetic studies of the intercalation of some organic compounds onto Na^{+}-montmorillonite. *Journal of Colloid Interface Science* **245**, 116–125.

Guo, Y. P. & Rockstraw, D. A., 2006 Physical and chemical properties of carbons synthesized from xylan, cellulose, and kraft lignin by H_3PO_4 activation. *Carbon* **44**, 1464–1475.

Gurses, A., Hassani, A., Kıransan, M., Acısli, O. & Karaca, S. 2014 Removal of methylene blue from aqueous solution using by untreated lignite as potential low-cost adsorbent: kinetic, thermodynamic and equilibrium approach. *Journal of Water Process Engineering* **2**, 10–21.

Ho, Y. S. & Mckay, G. 1998 The kinetics of sorption of basic dyes from aqueous solution by sphagnum mass peat. *Canadian Journal of Chemical Engineering* **76**, 822–827.

Kennedy, L. J., Vijaya, J. J. & Sekaran, G. 2004 Effect of two-stage process on the preparation and characterization of porous carbon composite from rice husk by phosphoric acid activation. *Industrial and Engineering Chemistry Research* **43**, 1832–1839.

Khan, A. R., Ataullah, R. & Al-Haddad, A. 1997 Equilibrium adsorption studies for some aromatic pollutants from dilute aqueous solutions on activated carbon at different temperatures. *Journal of Colloid Interface Science* **194**, 154–165.

Lagergren, S. 1898 About the theorie of so-called adsorption of soluble substances. *Kungliga Svenska Vetenskapsakademiens Handlingar* **24**, 1–39.

Langmuir, I. 1916 The constitution and fundamental properties of solids and liquids. *Journal of the American Chemical Society* **38**, 2221–2295.

Mas Haris, M. R. H. & Sathasivam, K. 2009 The removal of methyl red from aqueous solution using banana pseudo-stem fibers. *American Journal of Applied Sciences* **6**, 1690–1700.

Ozdemir, Y., Dogan, M. & Alkan, M. 2006 Adsorption of cationic dyes from aqueous solutions by sepiolite. *Microporous Mesoporous Material* **96**, 419–427.

Ravikumar, K., Krishnan, S., Ramalingam, S. & Balu, K. 2007 Optimization of process variables by the application of response surface methodology for dye removal using a novel adsorbent. *Dyes and Pigments* **72**, 66–74.

Reife, A. 1993 Dyes, environmental chemistry. In: *Kirk-Othmer Encyclopedia of Chemical Technology*. K. Othmer (ed), 4th edn, John Wiley & Sons, New York. pp. 753–784.

Santos, A. B. D., Cervantes, F. J. & Lier, J. B. V. 2007 Review paper on current technologies for decolorisation of textile wastewaters: perspectives for anaerobic biotechnology. *Bioresource Technology* **98**, 2369–2385.

Slimonin, J. P. 2016 On the comparison of pseudo-first order and pseudo-second order rate laws in the modeling of adsorption kinetics. *Chemical Engineering Journal* **300**, 254–263.

Sureshkumar, M. V. & Namasivayam, C. 2008 Adsorption behavior of Direct Red 12B and Rhodamine B from water onto surfactant-modified coconut coir pith. *Colloids and Surfaces A: Physicochemical and Engineering Aspects* **317**, 277–283.

Toth, J. 2000 Calculation of the BET-Compatible surface area from any type I isotherms measured above the critical temperature. *Journal of Colloid Interface Science* **225**, 378–383.

Tounsadi, H., Khalidi, A., Abdennouri, M. & Barka, N. 2016 Potential capability of natural biosorbents: *Diplotaxis harra* and *Glebionis coronaria* L. on the removal efficiency of dyes from aqueous solutions. *Desalination and Water Treatment* **57**, 16633–16642.

Tsai, F.-C., Ma, N., Chiang, T.-C., Tsai, L.-C., Shi, J.-J., Xia, Y., Jiang, T., Su, S.-K. & Chuang, F.-S. 2014 Adsorptive removal of methyl orange from aqueous solution with crosslinking chitosan microspheres. *J. Water Process Eng.* **1**, 2–7.

Wu, J. N., Eiteman, M. A. & Law, S. E. 1998 Evaluation of membrane filtration and ozonation processes for treatment of reactive-dye wastewater. *ASCE* **03**, 0272–0277.

Zarezadeh-Mehrizi, M. & Badiei, A. 2014 Highly efficient removal of basic blue 41 with nanoporous silica. *Water Resources and Industry* **5**, 49–57.

Zollinger, H. 1991 *Color Chemistry: Synthesis, Properties and Applications of Organic Dyes and Pigments.* VCH, New York.

First received 15 July 2017; accepted in revised form 1 October 2017. Available online 1 December 2017

Downloaded from http://iwaponline.com/jwrd/article-pdf/8/4/522/482431/jwrd0080522.pdf
by guest